Spatiotemporal gravity changes at Miyakejima Volcano, Japan: Caldera collapse, explosive eruptions and magma movement

Masato Furuya, Shuhei Okubo, Wenke Sun, Yoshiyuki Tanaka, Jun Oikawa, and Hidefumi Watanabe

Earthquake Research Institute, University of Tokyo, Tokyo, Japan

Tokumitsu Maekawa

Graduate School of Science, Hokkaido University, Sapporo, Japan

[1] Calderas are ubiquitous topographic features of volcanos, yet caldera formation itself has not been recorded intensively by modern measurement techniques. Here we report the spatiotemporal gravity changes before and after caldera collapse at the Miyakejima volcano, Japan in 2000. A gravity decrease of as much as 145 µGal (1 µGal = 10^{-8} m/s^2) at the summit area since June 1998 was detected 2 days prior to the collapse, interpreted as reflecting the formation of a large void beneath the volcano. Gravity changes detected after the initiation of collapse can mostly be corrected by the effect of collapsed topography, from which a rapid rate of collapse of more than 1.6×10^7 m^3/d can be inferred. Correcting for the effect of topography change, we identified a temporal decrease in gravity from the middle of July to late August despite ground subsidence. The gravity decrease is interpreted as a reduction of the density in a cylindrical conduit, attributed to water inflow from an ambient aquifer that also promoted intensive magma-water interaction and subsequent explosive eruptions. From September to at least November 2000, gravity values at all sites increased significantly by a degree that cannot be explained by ground displacement alone. We interpret this temporal evolution as primarily due to magma ascent and refilling of the conduit.   *INDEX TERMS:* 1208 Geodesy and Gravity: Crustal movements—intraplate (8110); 8414 Volcanology: Eruption mechanisms; 8434 Volcanology: Magma migration; 8439 Volcanology: Physics and chemistry of magma bodies; *KEYWORDS:* caldera collapse, void, hybrid microgravimetry, Miyakejima, Izu islands

1. Introduction

[2] Miyakejima is a basaltic stratovolcanic island in the Izu-Bonin arc, Japan (Figure 1). Historical records show that the volcano has erupted roughly every 20 years over the last few centuries [*Miyazaki*, 1984; *Tsukui and Suzuki*, 1998]. In the last decade, several institutes in Japan began monitoring the Miyakejima volcano, using seismometers [*Sakai et al.*, 2001; *Japan Meteorological Agency*, 2000; *Ukawa et al.*, 2000], tiltmeters [*Ukawa et al.*, 2000], magnetometers [*Sasai et al.*, 2001], and Global Positioning System (GPS) receivers [*Kaidzu et al.*, 2000; *Nishimura et al.*, 2001] and by levelling [*Tokyo Metropolitan Government*, 1990]. The activity at Miyakejima in 2000 notably involved the formation of a collapsed caldera, and this rare geological event was monitored intensively, providing a unique opportunity to investigate the dynamics of caldera formation and associated eruptions.

[3] The purpose of this paper is to report spatiotemporal gravity changes during the 2000 Miyakejima unrest and to propose a model that accounts for the observed gravity changes and crustal deformation to give insight into the caldera collapse mechanism and associated magma movement. The contents of this paper are as follows. In section 2, we describe the microgravimetry method employed in this study. In section 3, we divide the evolution of the 2000 Miyakejima unrest into four stages, and outline the volcanic activity and gravity changes in each stage. Subsequent sections are organized according to these four stages. Each section details the observed gravity changes and correlates the gravity data with the measured crustal deformation so as to form an unambiguous model and interpretation. Next, we describe the interpretation and modeling results and conclude with a discussion of the implications with respect to the mechanisms of caldera collapse, explosive eruptions, and magma movement.

2. Hybrid Microgravimetry

[4] Repeated microgravimetry measurement at an active volcano is a widely used technique that can reveal the redistribution of magma beneath volcanos by sensing
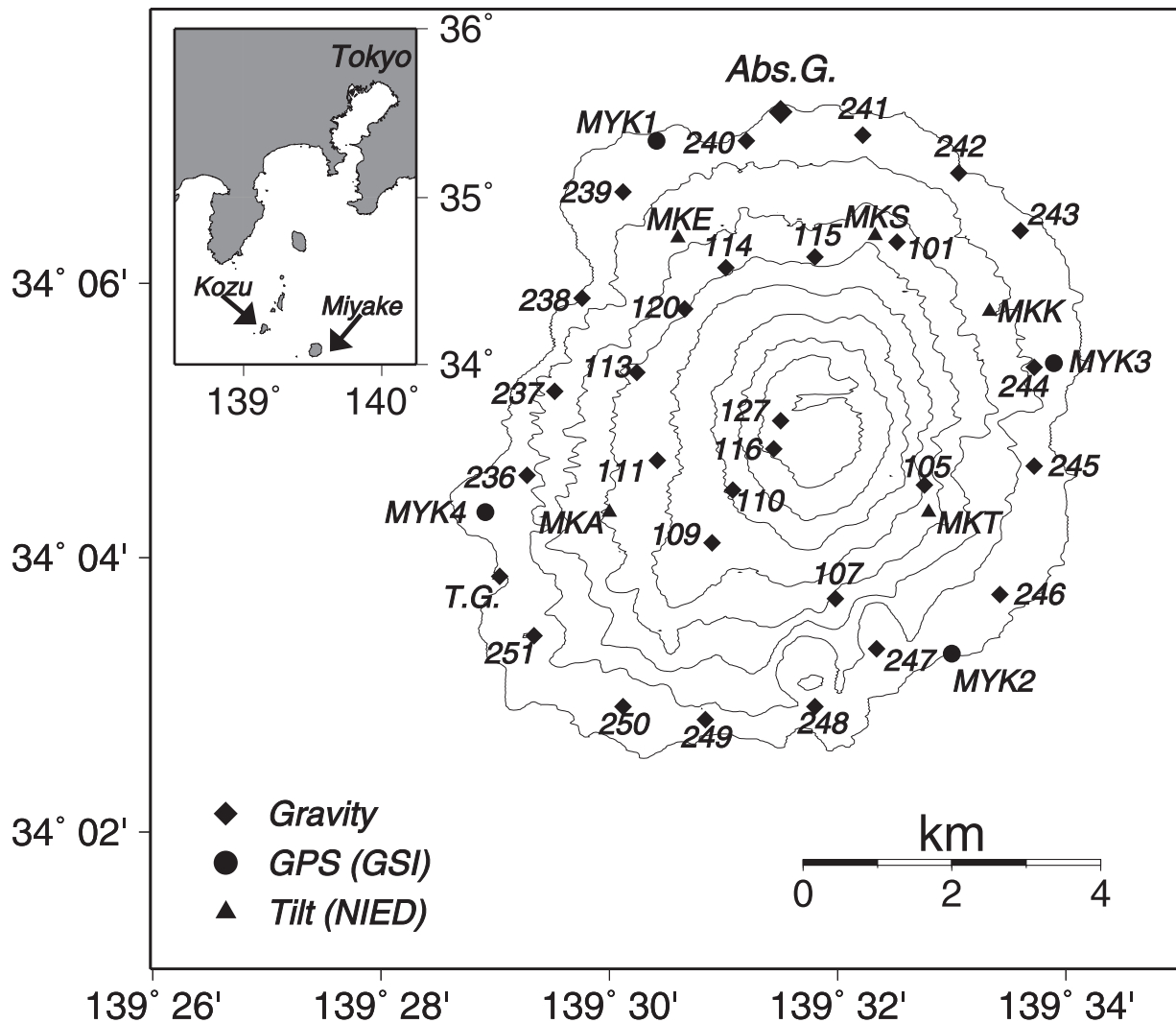
Figure 1. Map of Miyakejima volcano with contour interval of 100 m. Inset shows location of Tokyo, Miyakejima and Kozushima. Gravity measurement sites and bench marks are indicated by diamonds. Absolute gravity measurements were carried out at Miyakejima Weather Station (Japan Meteorological Agency). Also shown are the locations of four GSI GPS (circles) and five NIED tiltmeter (triangles) stations. See Figure A1 for temporal evolution of caldera collapse.

directly changes in the density distribution [*Jachens and Eaton*, 1980; *Dzurisin et al.*, 1980; *Okubo and Watanabe*, 1989; *Berrino et al.*, 1992; *Rymer et al.*, 1995; *Battaglia et al.*, 1999; *Gottsmann and Rymer*, 2002]. Conventionally, microgravity measurements have been carried out using relative gravimeters, which measure spatial changes with respect to a fixed reference site. To detect temporal changes, the absolute gravity at the reference site is assumed to be constant over time. However, on a small volcanic island such as Miyakejima, there is no guarantee of temporally constant gravity. For our measurements, we employed a state-of-the-art absolute gravimeter [*Niebauer et al.*, 1995], installed at the reference station in Figure 1. Other sites in Figure 1 were tied to the reference station, using two or three LaCoste-Romberg G-type gravimeters. We refer to this combined use of absolute and relative gravimeters as hybrid microgravimetry, and this technique allowed us to unambiguously record spatiotemporal evolution of gravity associated with the volcanic unrest. The absolute gravimeter

had an accuracy of the order of 1 μGal (1 μGal = 10^{-8} m/s^2). Although there are numerous reports on the gravity changes associated with earthquakes and volcanic unrest, *Tanaka et al.* [2001] were the first to report absolute gravity changes associated with an earthquake. To the best of our knowledge, this is the first report of absolute gravity changes associated with volcanic unrest.

3. Outline of the 2000 Miyakejima Volcanic Unrest

3.1. Stage 1: 26 June 2000 to Early July 2000

[5] A swarm of volcanic earthquakes in the evening of 26 June 2000 marked the onset of volcanic unrest after 17 years of quiescence [*Japan Meteorological Agency*, 2000; *Sakai et al.*, 2001]. The earthquake hypocenters migrated from the eastern to the western edge of the volcanic island over 12 hours. On 27 June 2000, changes in the color of the sea surface attributed to a small seafloor eruption were

observed on the west side of the island [*Nakada et al.*, 2001]. The hypocenters continued to migrate laterally toward the northwest for more than 20 km by 1 July 2000. The region beneath the volcano, on the other hand, exhibited virtually no seismicity until 4 July 2000.

[6] Four GPS stations of the Geographical Survey Institute (GSI) of Japan (Figure 1) recorded significant changes in disposition after the beginning of the earthquake swarm [*Kaidzu et al.*, 2000; *Nishimura et al.*, 2001]. Figure 2 shows the temporal changes in the three components of each position; data loss after September 2000 was due to an electrical outage. The most rapid changes occurred in the first week after the onset of unrest.

[7] Tiltmeters of the National Research Institute for Earth Science and Disaster Prevention (NIED) installed at the five stations in Figure 1 allowed us to observe the ground deformation with fine temporal resolution [*Ukawa et al.*, 2000]. The first tilt change occurred at MKT on the evening of 26 June 2000 with a downward tilt toward the east-northeast, indicating a swelling of the island. Two hours later, MKA exhibited the most dramatic downward tilt toward the south, reaching 0.16 mrad. Although other amplitudes were less than half that at MKA, the other tiltmeters also recorded changes that suggested a swelling of the island. However, the direction of tilt change at all meters changed from 28 June 2000, after which the tilt vectors indicated a subsidence in the western and southern parts of the island.

[8] A gravity-elevation change plot is shown in Figure 3 for the four stages of the 2000 unrest. The gradient of this plot can be used to interpret the processes occurring underground [*Gottsmann and Rymer*, 2002]. Since the elevation changes were not measured simultaneously at all gravity sites, four gravity sites located as close as possible to the GSI's GPS were selected, and the GPS data were used as a proxy of the elevation changes. The data marked with circles correspond to stage 1. Four other gravity sites that underwent subsidences of presumably greater than −60 cm are also plotted. The data for stage 1 deviate significantly from the Bouguer-corrected free-air gradient, which can be interpreted as a mass and density decrease [*Gottsmann and Rymer*, 2002].

3.2. Stage 2: Early July 2000

[9] Although the seismic swarm continued in the southeast, offshore of Kozushima (Figure 1), there was no seismic activity beneath the summit of the volcano after 28 June 2000 when the dike intruded offshore of Miyakejima. Many researchers considered that on the basis of their prior knowledge of the Miyakejima volcano, the 2000 volcanic unrest ended at that time. However, the number of earthquakes increased dramatically below the summit of the volcano from around 4 July 2000, lasting to the middle of August 2000. The hypocenters were distributed in a cylindrical volume with radius of about 500 m and extending 2500 m below sea level [*Sakai*, 2000].

[10] A small summit eruption occurred on the evening of 8 July, and ceased within 10 min. The collapse of the original topography at the summit was observed the following morning. Recognizable shapes such as a scoria cone generated in a 1940 eruption remained the same, and the northern area remained covered with vegetation [*Nakada et al.*,

2001]. The appearance strongly suggested that the collapse was caused by implosion rather than explosion. The eruption deposits surrounding the collapsed caldera at that time were estimated to total only 1.5×10^5 tons [*Nakada et al.*, 2001], which is an order of magnitude smaller than the collapsed volume. The summit eruption on the evening of 8 July marked the initiation of caldera collapse.

[11] The growth rate of caldera collapse was most rapid in the initial stage after the first small summit eruption on 8 July 2000 and gradually eased from the middle of August to September 2000. Remarkably, the caldera growth was not accompanied by eruptions that could generate eruptive material comparable to the caldera volume.

[12] Gravity changes detected immediately after the collapse amounted to as much as −1135 μGal, suggesting a rapid rate of caldera collapse. The data marked with triangles in Figure 3 correspond to stage 2 and have been corrected for the effect of topography changes due to the caldera collapse. As in stage 1, the data suggest a mass and density decrease.

3.3. Stage 3: Middle July 2000 to September 2000

[13] Explosive summit eruptions first occurred on 14 and 15 July 2000 followed later by eruptions on 10 August and explosive phreatomagmatic summit eruptions on 18 and 29 August 2000. The eruption on 18 August 2000 was the largest; the plume top reached as high as 15 km. Such explosive summit eruptions have been uncommon for Miyakejima over the past few centuries, raising the question as to what controls the explosivity at Miyakejima.

[14] Notable observations during this stage are a long-period seismic pulse [*Kumagai et al.*, 2001] and step-wise changes in both tilt [*Ukawa et al.*, 2000] and electric field [*Sasai et al.*, 2001], which began after the onset of caldera collapse. All these changes occurred simultaneously once or twice per day and were shown to correlate with the tides [*Kasahara et al.*, 2001]. These characteristic signals, however, have not been observed since the largest eruption on 18 August 2000. Besides these long-period signals, normal shorter-period earthquakes also occurred beneath the collapsed caldera. The hypocenter distribution was cylindrical as noted above. The migration of earthquake hypocenters from Miyakejima toward Kozushima detected in late June 2000 was not detected from July to August, although the earthquake swarm to the east and southeast offshore of Kozushima continued.

[15] The crustal deformation also continued, and the rate of subsidence and contraction in the island remained almost the same through to September 2000 (Figure 2). Correcting for the effect of topography changes due to caldera collapse on gravity changes, we found that gravity values did indeed decrease in this stage, as plotted in Figure 3. The deviations from the Bouguer-corrected free-air gradient suggest mass and density decreases as in stages 1 and 2 [*Gottsmann and Rymer*, 2002].

3.4. Stage 4: After September 2000

[16] Although a white vapor plume has emitted continuously from the vent, large-scale explosive eruptions have not occurred since 29 August 2000. The frequency of earthquakes beneath the volcano have also dramatically decreased. Since September 2000, however, volcanic gas,
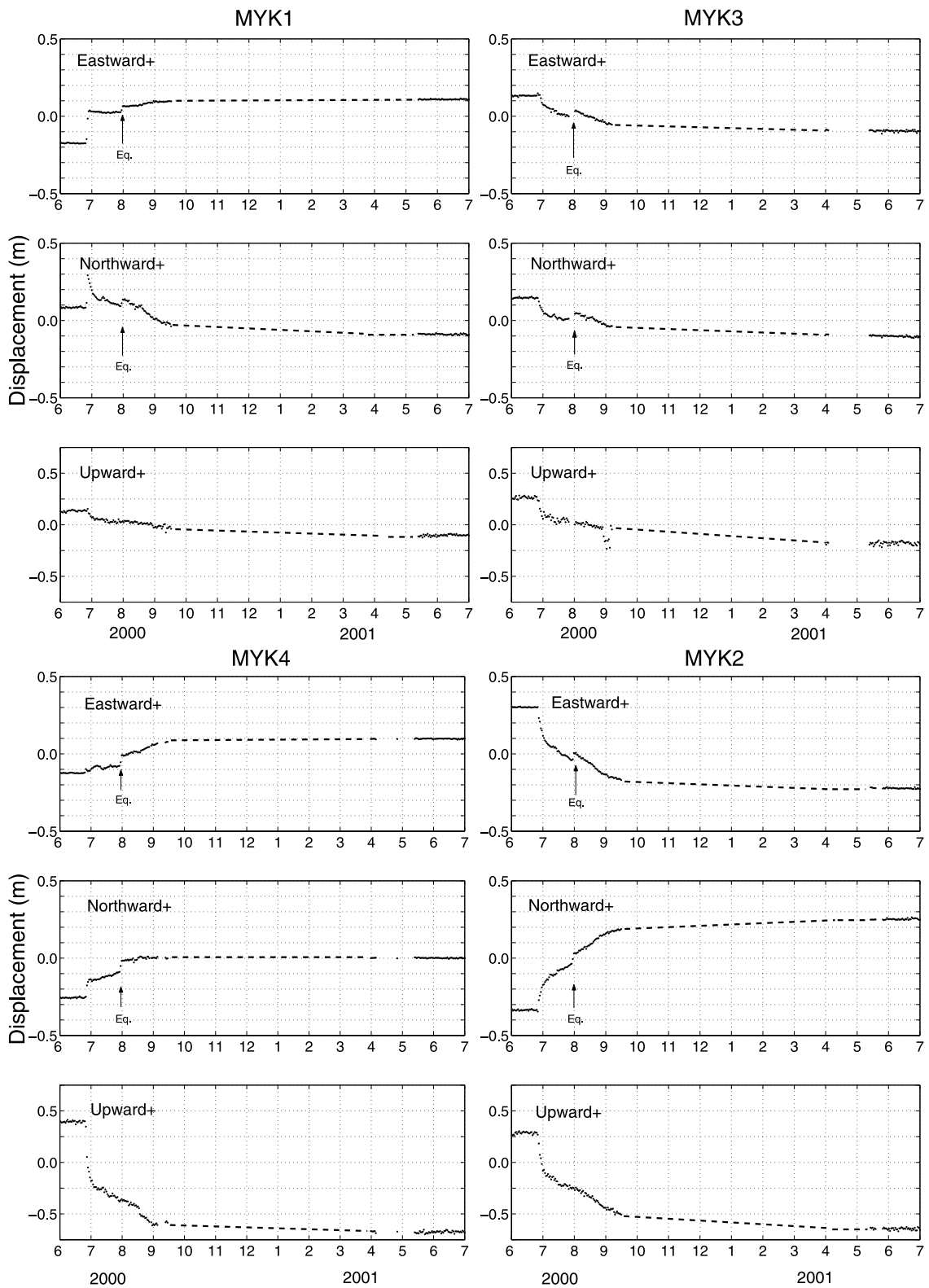
Figure 2. Temporal changes in site positions of GSI GPS (locations shown in Figure 1). Largest coseismic change is indicated by arrow. Each panel is displayed to conform to the location on the volcanic island. Because of an electrical outage, data continuity is lost from September 2000. (Copyright of original data is retained by the Geographical Survey Institute of Japan.)
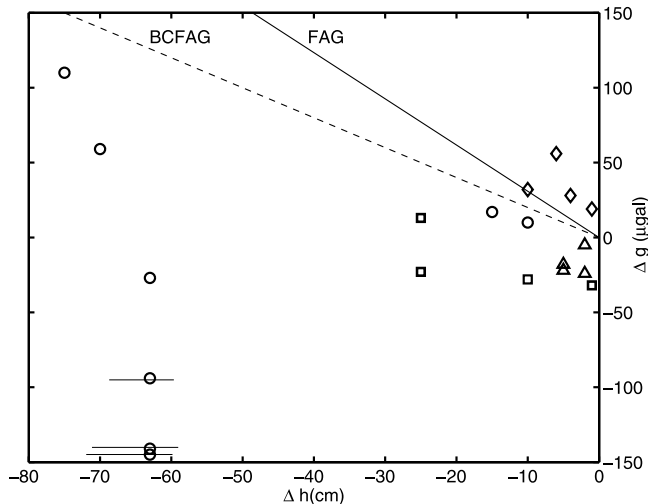
Figure 3. Gravity and elevation changes for the four stages; (1) June 1998 to early July 2000 (circles), (2) early July (triangles), (3) mid-July to late August 2000 (squares), and (4) September–November 2000 (diamonds). For the first stage, four other gravity measurements are also shown, representing sites that subsided presumably greater than 60 cm. FAG and BCFAG represent the free-air gradient (-3.086 μGal/cm) and Bouguer-corrected free-air gradient (-2.00 μGal/cm), respectively. The distinctly different clusters for each stage reflect the different processes as discussed in the text.

in particular sulfur dioxide (SO_2), has been discharging at unprecedented volumes. The SO_2 emission rate gradually increased from September to December 2000 and exceeded 4.8×10^4 t/d on average from September 2000 to January 2001 [*Kazahaya et al.*, 2001]. The huge amount of gas discharge has prevented the evacuated residents of the island from returning for more than a year. The Japan Meteorological Agency (JMA) has been monitoring temperatures near the volcanic vent by infrared thermometer from a helicopter, revealing that the temperature increased to 400°C by January 2001. The measured temperature is probably lower than the actual temperature because the vent itself is often masked by the vapor plume and dust. JMA also reported a volcanic glow at nights from December 2000 to January 2001.

[17] The electrical outage since September 2000 has prevented the GSI from continuously monitoring crustal deformation. According to the four single-frequency GPS receivers temporarily installed by JMA on October 2000, the ground contraction appeared to be continuing. The contraction since September 2000, however, seemed to cease around April–May 2001, as indicated by the baseline changes recorded by JMA's GPS. On the basis of this observation, we linearly interpolated the GSI's GPS data with the measurements resumed in April and May 2001 (Figure 2). The rate of contraction and subsidence certainly slowed from September 2000, as most clearly observed in the north-south component of MYK1 (Figure 2). The rate of horizontal displacement is at most 1 cm/month. The displacement at MYK4 is the smallest recorded by any of the GPS sites.

[18] The gravity changes detected in stage 4 deviate systematically and significantly from the free-air gradient (Figure 3), which suggests mass and density increases [*Gottsmann and Rymer*, 2002]. The distinctly different clusters for each stage in Figure 3 reflect the different processes as discussed in detail below.

4. Dike Intrusion and Events Contributing to Caldera Collapse

4.1. Observation Results

[19] Figures 4a and 4b show the cumulative ground displacements from 26 June to 6 July 2000. For the north-south component at MYK1, we have taken the maximum displacement to 6 July 2000, considered to be caused by dike intrusion as discussed below and used it to estimate the widening of the tensile crack. The style of deformation was spatially inhomogeneous. As suggested from Figure 2, the north-south baseline on the western side of the island extended as much as 20 cm in the first 3 days. Although not clearly observable in Figure 2, baseline extension of up to 3 cm was also recognized on the eastern side of the island. From 28 June 2000 on, all four stations began indicating a contraction of the island. This change of deformation style was also detected by tilt changes as noted above. The amplitude of ground subsidence also varied between sites (Figure 2). The southern part of the island subsided significantly in comparison to the northern part. MYK2 and MYK4 subsided as much as 40 and 70 cm, respectively, while MYK3 subsided at most 15 cm. Although MYK1 exhibited significant changes in horizontal components, the height changes were not as significant as at other locations, and the total subsidence to 6 July 2000 was evaluated to be 10 cm. The rate of subsidence at MYK1 slowed gradually over time.

[20] A university team carried out a GPS campaign on August 1999 and 2 July 2000. The station located close to gravity site 109 in the middle of the flank of the island (Figure 1) recorded a subsidence of 63 ± 10 cm shown in Figure 3. Unfortunately, the GPS receiver in the summit caldera was lost in the caldera collapse.

[21] Figure 4c shows the changes in gravity obtained by the survey for the periods 2–5 June 1998 and 2–6 July 2000. The detected gravity changes vary spatially, and are far from isotropic. A large gravity decrease of as much as -145 ± 10 μGal occurred around the summit on 6 July, 2 days before the onset of collapse. At one site in the southwest of the island, we detected a localized increase of $+110 \pm 10$ μGal, and at a couple of sites in the southeastern area of the island, we detected regional increases of as much as $+60 \pm 10$ μGal. It should also be noted that the absolute gravity at the reference site exhibited a significant increase of $+10 \pm 1$ μGal.

4.2. Interpretation and Modeling

[22] As clearly indicated by the tilt changes and earthquake hypocenter locations, the first change associated with the 2000 unrest was detected on the south side of the summit. We interpret this as the beginning of a decompression inside a magma chamber in this area, and the gravity increase detected in the southern part of the island is explained by a point deflation source in this area [*Mogi*, 1958; *Hagiwara*, 1977]. The optimum location and depth are estimated below.
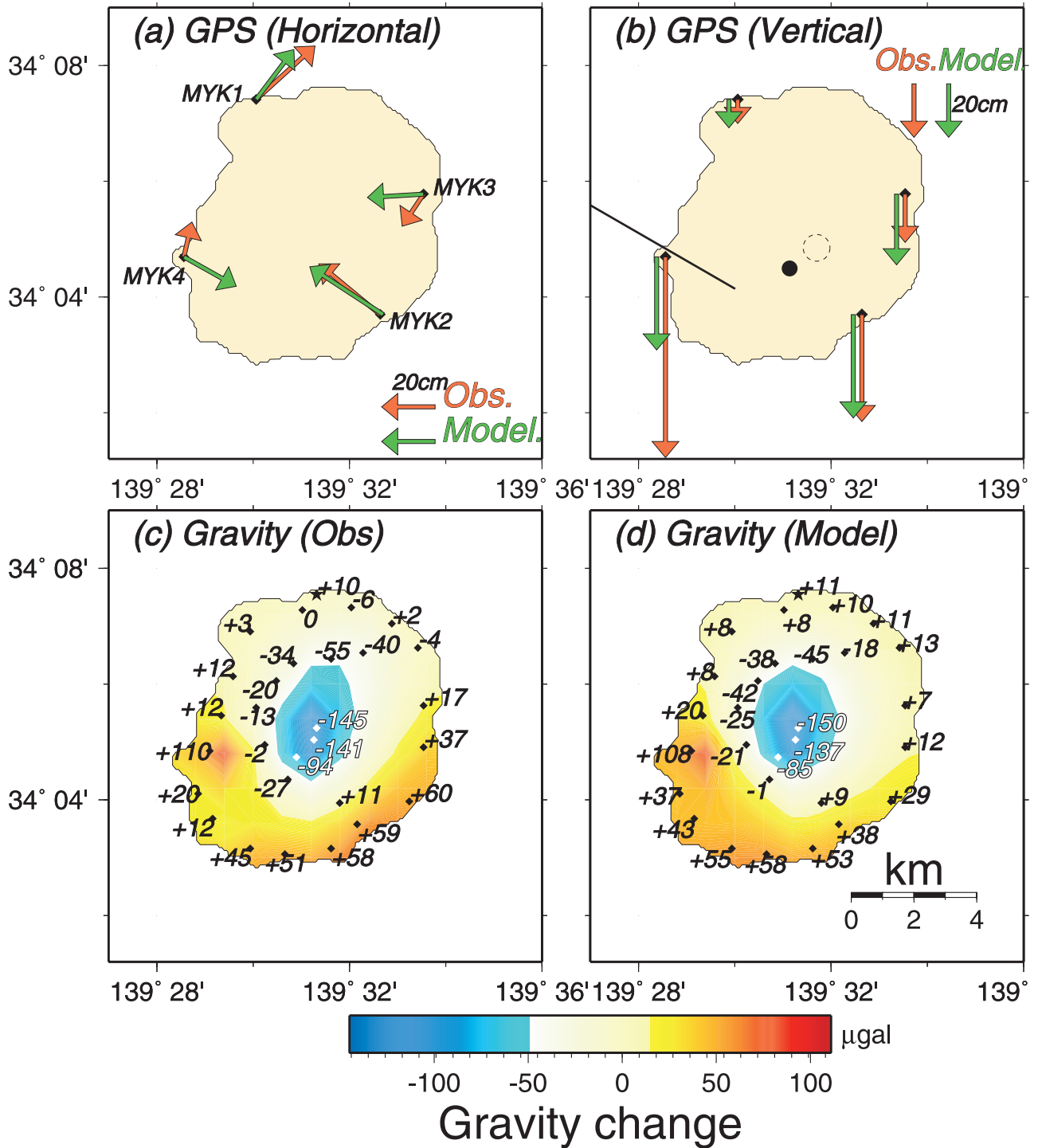
Figure 4. (a) Horizontal component of GPS displacement field obtained by GSI from 26 June to 6 July 2000. Northward displacement of MYK1 was obtained to 28 June 2000 (see text). (b) Vertical component of GPS displacement. Horizontal locations of void and deflation source are shown with dashed and solid circles, respectively. The strike of tensile dislocation is also shown. (c) Gravity changes from 5 June 1998 to 6 July 2000, 2 days prior to summit collapse. Units are in microGals (= 10^{-8} m/s^2). The star and solid dots designate measurement points of absolute and relative gravimetry, respectively. (d) Computed gravity changes based on the optimum model. See also Figure 5 and Table 1.

[23] In view of the migration of earthquake hypocenters, the lengthening of the north-south GPS baseline in the west, and the large tilt changes in the southwest site noted above, it is considered that a dike intruded on the southwestern edge of the island on 27−28 June 2000. The localized gravity increase at the southwestern site was presumably caused by this dike intrusion and subsequent ground subsidence. In modeling the detected changes in gravity and
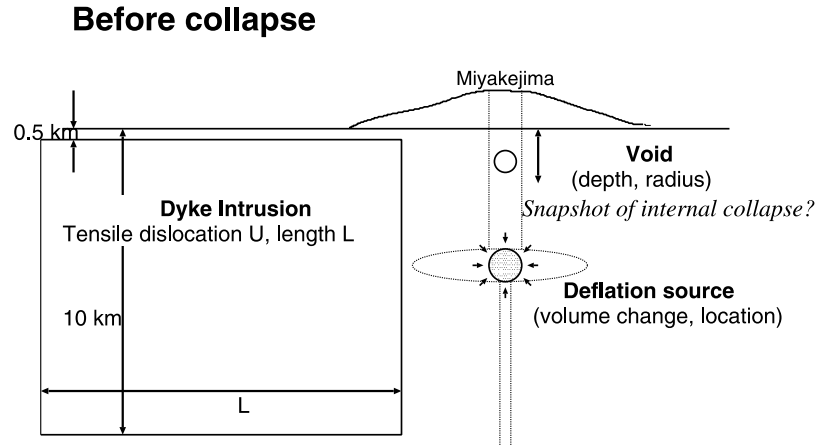
Before collapse

Figure 5. Three-element model: void, rectangular dike, and deflation source, accounting for the observed gravity changes and ground displacements immediately prior to the collapse.

ground displacement, we employ analytical expressions for ground displacement [*Okada*, 1985] and gravity changes [*Okubo*, 1992] due to a tensile dislocation.

[24] A large decrease in gravity in the summit area was detected 2 days prior to the summit collapse. Although negative gravity changes are usually regarded as indicating ground uplift, the GSI GPS measurements revealed a contraction and subsidence at that time and the university team's GPS near gravity site 109 on the southwestern flank of the volcano indicated a significant subsidence. Hence it is highly unlikely that the summit area uplifted locally. Considering the summit collapse that occurred on 8 July, with very little associated eruption deposits and the appearance noted above, the source of this negative gravity change is thought to have been an empty space beneath the volcano. This is further supported by the total magnetic intensity changes detected from 26 June to 10 July 2000 close to the summit, which can be modeled by a perfect demagnetized sphere [*Sasai et al.*, 2001]. A simple empty sphere is used to represent the decrease in density without exerting stress around the medium that would cause uplift at the surface.

[25] In order to account for the ground displacements and gravity changes in Figures 4a, 4b, and 4c, we developed a source model consisting of a deflation source, a tensile dislocation, and an empty sphere (Figure 5) and estimated some of the relevant physical parameters. In the joint inversion, we minimized the following quantity, L:

$$ L = \sum_{i=1}^{29} \left(\frac{g_i^{obs} - g_i^{cal}}{Wg_i} \right)^2 + \sum_{i=1}^{4} \left(\frac{\overrightarrow{d_i^{obs}} - \overrightarrow{d_i^{cal}}}{Wd_i} \right)^2, \quad (1) $$

where Wg_i and Wd_i are assigned weights for the ith site. The weight for gravity data was set at 10 μGal and 2 μGal for the absolute gravimeter, while the weight for the GPS data was set at 2 cm. Optimum parameters were obtained by the simplex algorithm [*Press et al.*, 1992].

[26] The optimized and prescribed source parameters are listed in Table 1, and the horizontal locations are shown in Figure 4b. The height and strike of the dike were fixed in accordance with the hypocenter distributions [*Sakai et al.*, 2001]. Computed ground displacement and gravity changes

are shown in Figures 4a, 4b, and 4d. The optimized model adequately explains the overall observed changes. The deflation source is estimated to be located to the south of the summit, as speculated above. The estimated depth of the empty cavity is consistent with that estimated from the measurement of total magnetic intensity changes [*Sasai et al.*, 2001]. In order to explain some discrepancies in the gravity changes in the southeastern area and ground displacements in the southwestern area, a more complex source model is necessary.

5. Initiation of Caldera Collapse

5.1. Observation Results

[27] GSI carried out airborne photogrammetry on 9 July 2000 and constructed a digital terrain model (DTM), bring-

Table 1. Optimum Model Parameters for Figure 4

Parameter	Value
Deflation Source	
Medium density,[a] kg/m³	2,600
Longitude	139°31′9″ ± 3″
Latitude	34°4′30″ ± 3″
Depth, m	5,300 ± 450
Volume change, m³	−8.7 ± 0.5 × 10⁷
Void	
Medium density,[a] kg/m³	−2,300
Longitude	139°31′42″ ± 3″
Latitude	34°4′51″ ± 3″
Depth, m	1,740 ± 200
Radius, m	240 ± 20
Tensile Dislocation	
Longitude[b]	139°22′15″
Latitude[b]	34°7′49″
Strike direction[b]	N60°W
Dip angle[b]	90°
Open dislocation, m	1.6 ± 1.0
Length, m	13,500 ± 1,000
Bottom depth,[b] m	10,000
Depth to the top,[b] m	500
Density contrast,[b] kg/m³	0

[a]Density inside the medium is fixed [*Fujii and Kushiro*, 1977].
[b]Fixed parameters. For tensile dislocation, the position of the western edge is shown.
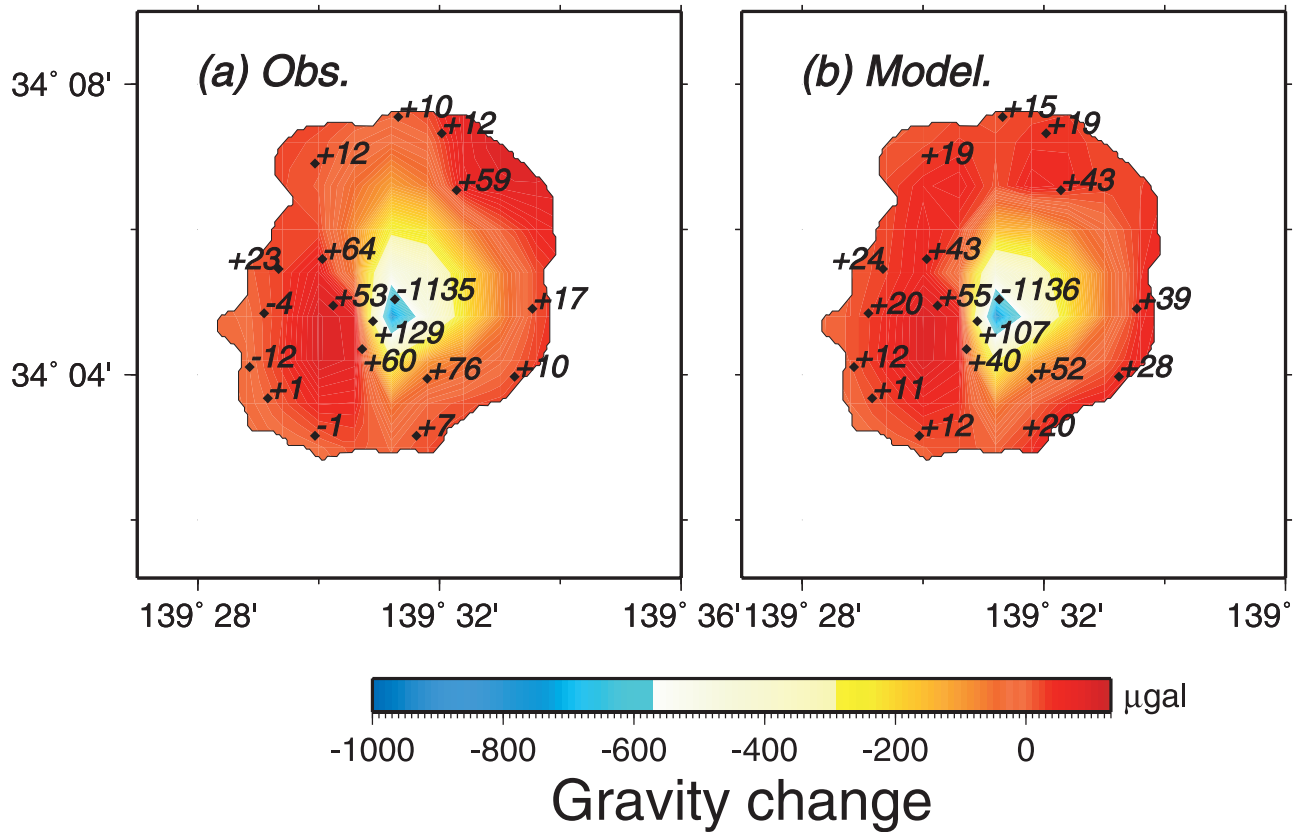
Figure 6. (a) Gravity changes at Miyakejima from 1–6 July to 11–14 July 2000, before and after the summit collapse. (b) Computed gravity changes based on the collapsed topography model. See Figure 7.

ing to a total of 8 the DTMs constructed for different periods to January 2001 [*Hasegawa et al.*, 2001]. We made use of these to synthesize a digital elevation map for the whole island as discussed in Appendix A. Our estimates of the collapsed volumes on 9 and 22 July are 5.77×10^7 m^3 and 28.0×10^7 m^3, respectively. A simple linear interpolation gives a collapse rate of 1.7×10^7 m^3/d, but the rate is expected to be much higher in the initial stages. It should be noted, moreover, that the volume of erupted material surrounding the caldera to 15 July 2000 is estimated to be 2.2×10^6 m^3 [*Nakada et al.*, 2001], which is an order of magnitude smaller than the caldera volume. In other words, caldera growth proceeded with a very small amount of erupted material. Therefore the mass of the original topography must have disappeared beneath the ground. We can regard the gravity changes due to the eruption deposits outside the caldera as negligible.

[28] Gravity changes after the initiation of caldera collapse are shown in Figure 6a. These changes are derived from measurements taken between 2–6 July and 11–14 July 2000. An extraordinary large decrease exceeding -1000 μGal near the caldera rim and a significant increase in the middle of the flank were recorded on 11 July. Measurements at most of the sites near the coast were conducted on 14 July 2000.

[29] Figure 2 shows that the rate of ground subsidence and contraction was almost constant from 1 July to the middle August 2000 except for coseismic changes [*Nishimura et al.*, 2001]: the subsidence rate of MYK1 and

MYK3 was 0.25 ± 0.02 cm/d, while that for MYK2 and MYK4 was 0.68 ± 0.02 cm/d. According to the GPS data obtained by the university team, ground displacements on the flank of the island between the two periods, 2–6 July and 11–14 July 2000, were within measurement uncertainty, and subsidence was less than 3 cm (T. Matsushima, personal communication, 2000), which is roughly consistent with the rate inferred from GSI's GPS measurements.

5.2. Interpretation and Modeling

[30] Since the direct attraction of the topographic mass was lost due to the dramatic change of topography during initiation of caldera collapse, gravity values will have increased at some sites and decreased at others, depending on the relative height of each gravity point with respect to the caldera volume. Although many effects contributed in reality as argued below, Figure 6a suggests that this mass-loss effect is dominant in the measurement results. Because of the disappearance of the original topography, downward attraction was lost near the summit, causing a decrease in gravity (-1135 μGal). In contrast, at the sites on the middle of the flank of the volcano, upward attraction is lost, and we can expect an increase in gravity of as much as 140 μGal.

[31] For the moment, we suppose that the gravity changes in Figure 6a are explained entirely by the loss of topographic mass, and ignore the effects of crustal deformation and density changes. These additional effects are discussed below. Under this assumption, we first examined how the

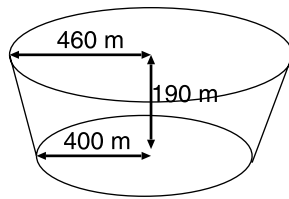## Collapsed topography model for 11 July 2000

Figure 7. Collapsed topography model for 11 July 2000 accounting for the gravity changes immediately following summit collapse. The difference between the radii of the upper and lower edges is inferred from photographs of the summit collapse.

DTM on 9 July 2000 accounts for the gravity changes, using the original DTM before the collapse as a reference (see Appendix A). We found that the DTM on 9 July 2000 explains only −90 μGal at the largest negative change in Figure 6a, assuming a density of 2300 kg/m^3 for the collapsed topography. For the site where the largest positive change was detected in Figure 6a, the DTM accounted for 70 μGal. The DTM on 9 July 2000 obviously fails to explain the results in Figure 6a.

[32] We can attempt to explain the largest negative and positive changes in Figure 6a most simply by supposing a much larger collapsed volume. Considering that the collapse proceeded most rapidly in the initial stages, it is plausible that the volume collapsed by 9 July 2000 when the DTM was obtained is smaller than the actual volume on 11 July 2000. Gravity change data near the coastline were acquired on 14 July, and therefore we may have to develop another model to explain those data. However, in order to explain the large gravity changes near the caldera rim and in the middle of the flank and the rate of collapse in the very initial stage, we developed a collapsed topography model based primarily on the larger gravity changes obtained on 11 July 2000 (Figure 7).

[33] Computed gravity changes are shown in Figure 6b. In the computation, we employed an analytical formula for the gravity of a cylindrical body [*Singh*, 1977] and approximated the shape in Figure 7 as stacked thin circular disks. The difference in the radius of the upper and lower edges is inferred from the photographs of summit collapse. The model collapse volume is 11.0×10^7 m^3. Comparing the estimate with the collapsed volume as of 9 July 2000, the collapse rate appears to be 2.6×10^7 m^3/d, which is higher than the simple estimate in section 5.1 and is consistent with the expectation that the collapse was most rapid in the first stages.

[34] We then consider reevaluation of this model taking into account the other effects. The effect of crustal deformation will increase the gravity values at all sites because the entire island was undergoing ground contraction and subsidence at that time. Thus the collapsed topography should induce a large negative gravity change near the caldera rim and a smaller positive change in the middle of the flank. Therefore we will have to suppose a larger radius at the top and a smaller radius at the bottom of the collapsed topography model (Figure 7). However, the volume of the collapsed topography is not expected to differ significantly from the estimate above because the ground displacement between the measurement periods was rather small.

[35] If the density changes occur above sea level, gravity values at some sites will increase and those at others will decrease. There is no evidence in the period immediately following the initiation of caldera collapse to suggest the ascent of magma above sea level. Thus it is unlikely that the density increase occurred somewhere above sea level. In contrast, in view of the ongoing collapse it is likely that negative density changes occurred above sea level. However, it is difficult to distinguish this effect from that of collapsed topography, and thus we will suppose that this effect, if any, is included in the collapsed topography model derived above. As discussed in the next section, it is also likely that some part of the density decrease occurred below sea level. If so, we will have to suppose a smaller radius at the top and a larger radius at the bottom of the collapsed topography model. There is no evidence to suggest, however, that the radius at the bottom of the collapsed caldera was greater than that at the top. If the density increased below sea level, it would cause all gravity values to increase, and it would be necessary to reexamine the estimate. However, we will discuss later that magma flowed out laterally at depths below sea level in this period, and we consider that it is unlikely that the effect of density increase below sea level dominates other effects.

6. Caldera Growth and Explosive Summit Eruptions

6.1. Observation Results

[36] Figure 8 shows temporal gravity changes at the reference absolute gravity point on 6 June 2001. Also shown are the effects of topography change due to caldera collapse. All other sites exhibited similar behavior (see auxiliary material[1]). The effects of mass loss due to caldera collapse were estimated using the synthetic DTM as discussed in Appendix A. As crustal deformation was not measured at all gravity points, those data are not shown. The observed gravity corrected for topography change in Figure 8 therefore reveals the effects of both crustal deformation and density changes above and below sea level.

[37] Despite the ground contraction and subsidence, the corrected gravity changes exhibited a significant temporal decrease from July to the middle of August, particularly at northern sites (Figures 3 and 8); the larger the assigned density of topography, the greater the gravity decrease. It should also be noted that the period of temporal decrease coincides with the period of intermittent explosive eruptions and slowing caldera growth. Figure 9 shows the ground displacements (Figures 9a and 9b) and corrected gravity changes (Figure 9c) from 11 July to 12 August 2000 assuming a density of 2300 kg/m^3 for the collapsed topography. A number of measurement sites were inaccessible due to the intermittent explosive eruptions. As expected from Figure 8, a temporal gravity decrease can be seen, most notably over

---

[1] Auxiliary material is available via Web browser or Anonymous FTP from ftp://ftp.agu.org, directory "append" (Username = "anonymous", Password = "guest"); subdirectories in the ftp site are arranged by paper number. Information on searching and submitting electronic supplements is found at http://www.agu.org/pubs/esupp_about.html.
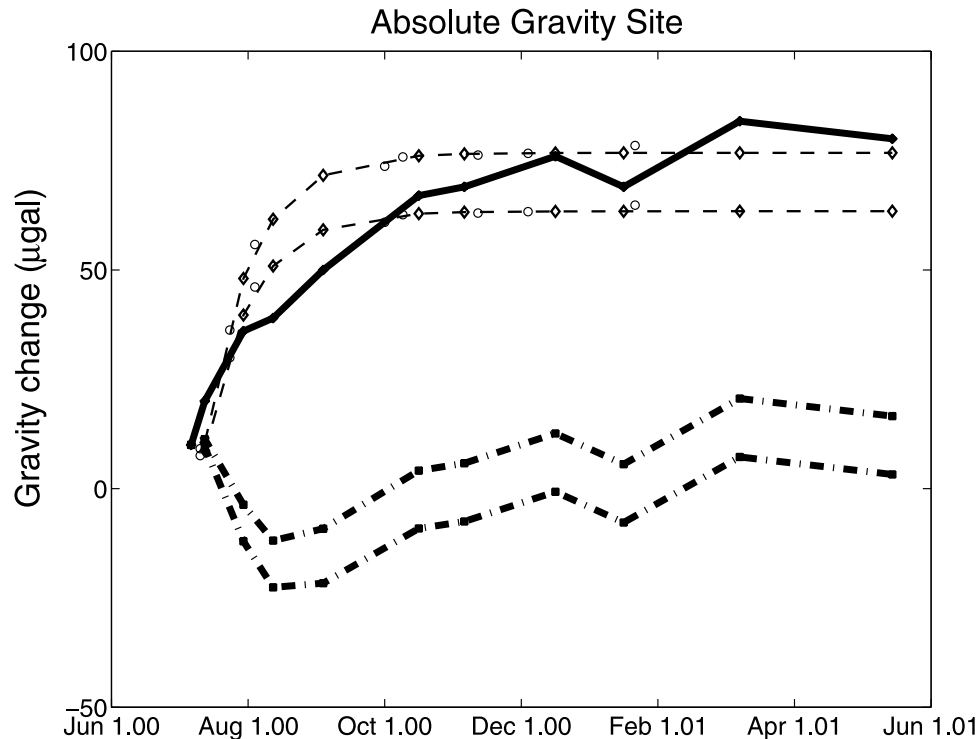
Figure 8. Temporal changes of observed absolute gravity (thick solid line), effect of collapsed topography (dashed line) and the corrected gravity (dash-dotted line) since June 1998. Gravity changes from 979,799,740 μGal are shown. Measurement error of absolute gravity is 1 μGal, while that for relative gravity is 10 μGal. The collapsed topography model is based on our synthetic digital elevation maps originally developed by GSI for the summit area at several dates denoted by open circles [*Hasegawa et al.*, 2001]; see also Appendix A. The effects of collapsed topography are temporarily interpolated to estimate the expected gravity changes on the dates of gravity measurements, denoted by diamonds. We assumed two values of density, 1900 and 2300 kg/m^3 as end-members. The larger the density value, the larger the predicted changes.

the northeastern area where ground subsidence was less than 10 cm (Figure 9b). Meanwhile, the southern region undergoes a larger crustal subsidence of as much as 30 cm (Figure 9b), causing an increase in gravity. If the actual density of collapsed topography is less than 2300 kg/m^3, the temporal gravity decrease will not be so large. As shown in Figure 8, however, the temporal decrease in gravity can still be observed at a number of sites even if the density of collapsed topography is assumed to be 1900 kg/m^3.

6.2. Interpretation and Modeling

[38]   The gravity changes in Figure 9c should be due to the effects of crustal deformation as well as density changes beneath the ground. The crustal deformation causes the gravity values to increase as noted above. Nevertheless, we see a gravity decrease in the northern and northeastern areas. The effect of density decrease therefore appears to exceed that of crustal deformation, and the results indicate that a significant reduction in density sufficient to mask any gravity increase due to ground subsidence occurred during that period.

[39]   In order to account for the inferred gravity changes as well as the ongoing crustal deformation, we developed a model consisting of two point deflation sources and a cylindrical body lighter than the surrounding medium (Figure 10). We employ a cylindrical body to conform to

the distribution of hypocenters; *Kumagai et al.* [2001] also employed a cylindrical piston to explain the long-period seismic pulse. The GPS displacement is explained only in terms of the point deflation sources. Note that the cylindrical body does not exert any stresses around the medium and thus causes no ground displacement. To compute the gravity due to the cylindrical body, we used an analytical formula presented by *Singh* [1977]. As a model to account for the ground contraction and subsidence and consequent gravity increase, we used the point source model of *Mogi* [1958] and *Hagiwara* [1977]. Figures 9a and 9b show larger horizontal and vertical movements in the southern part of the island that cannot be reproduced well by a single isotropic point source; this is also true for gravity changes. We failed to derive a physically plausible estimate when we assumed one deflation source and a closing tensile dislocation. Two deflation sources could adequately reproduce the observed GPS displacements.

[40]   Joint inversion was carried out in the same way as in section 6.1, by minimizing a quantity such as equation (1). Here, however, the weight for gravity data is set at 20 and 5 μGal for the absolute gravimeter, considering the errors in our estimate of collapsed topography corrections in addition to measurement error. The weight for GPS data is set at 5 cm, considering the errors in the corrections of the coseismic effect.
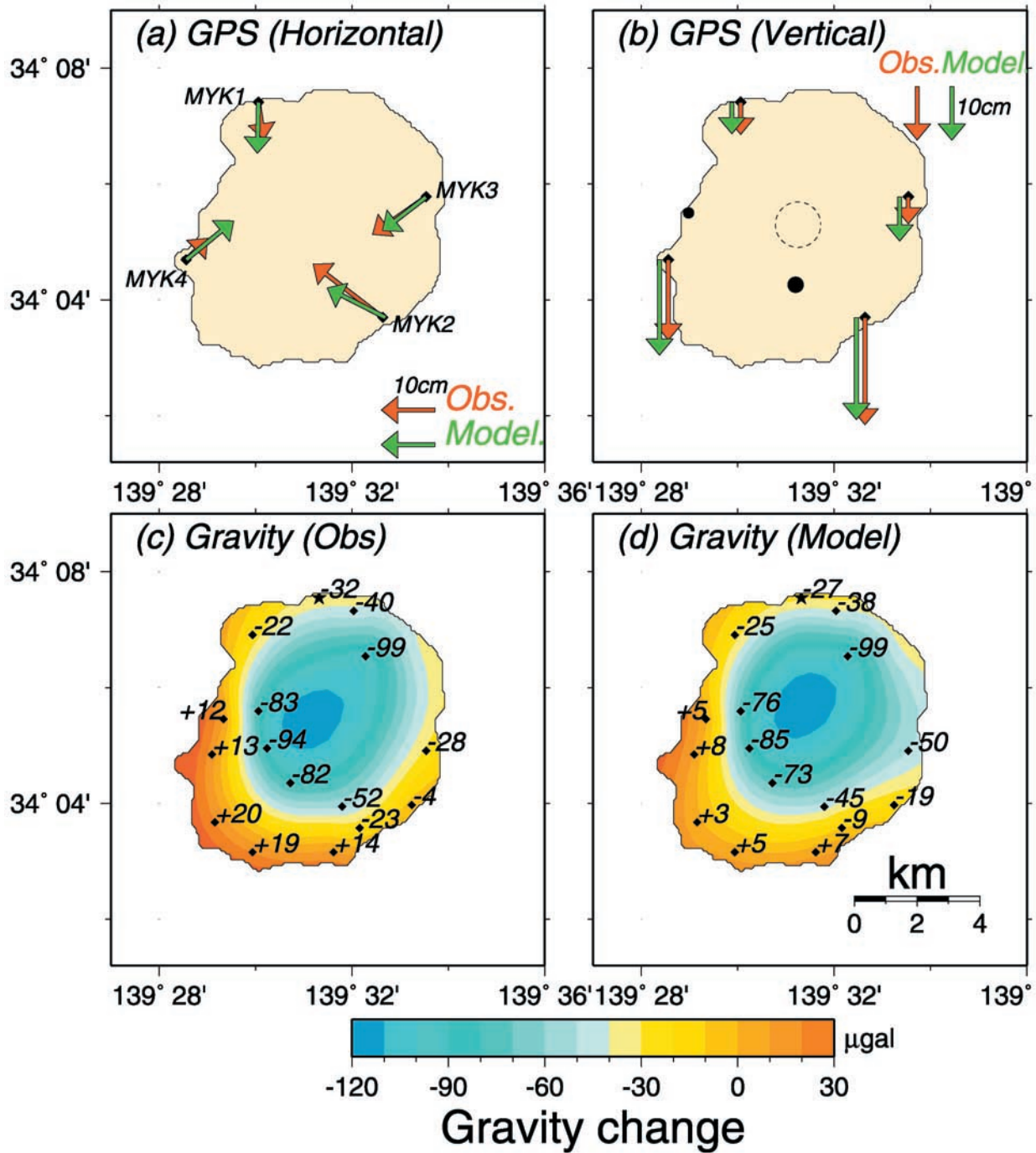
Figure 9. (a) Horizontal component of GPS displacement field derived by GSI from 11–14 July to 10–12 August 2000. (b) Vertical component of GPS displacement. (c) Gravity changes acquired from 11–14 July to 10–12 August 2000. Units are in microGals. The effect of collapsed topography has been corrected, assuming a density of 2300 kg/m^3. The reference site is located at the northernmost point, as designated by a star. (d) Computed gravity changes based on the optimum model. See Table 2.

[41] Computed ground displacement and gravity changes are shown in Figures 9a, 9b, and 9d. Optimum model parameters are listed in Table 2, and the locations of the deflation sources are indicated in Figure 9b. The estimated size of the cylindrical body conforms to the seismicity map for the region beneath the volcano in this particular period. We interpret the event as a collapse of the preexisting cylindrical structure and an inflow of water from an ambient aquifer, resulting in a significant reduction of the density of the cylindrical body. Although the larger deflation source moved upward, its horizontal location was estimated to be close to that listed in Table 1 (see also Figure 4b), suggesting a more complex source system in reality.

[42] The explosive summit eruption was presumably caused by the interaction of water with magma or hot rock within the central conduit. As discussed later, a number of
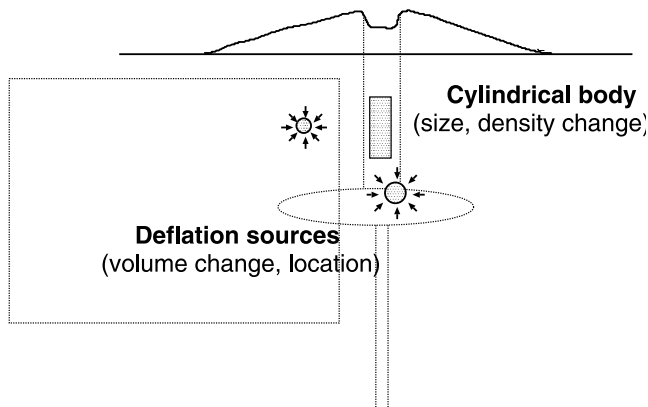
During explosive eruption

Figure 10. Source model accounting for both the observed gravity changes and ground displacements during explosive eruptions. Two deflation sources were employed to explain ground displacements. To explain the gravity decrease, we assumed a cylindrical body that underwent a density decrease. We take the cylindrical form to conform to the hypocenter distribution [*Sakai*, 2000]. See text for details.

observation suggest the involvement of magma, such as early gravity increases attributed to a rising magma column, increasing temperatures near the vent, observations of volcanic glow in December 2000, and increased SO_2 emission from September to December 2000.

7. Discharge of Volcanic Gas

7.1. Observation Results

[43] Gravity changes since September 2000 are also shown in Figure 8. Notably, the corrected gravity values at all sites began to increase after September 2000 up until at least November 2000. Large changes in gravity were detected at sites close to the caldera. The largest increase in gravity to May 2001 was observed at site 107. The rate of gravity change decreased from November to December 2000 to close to the limit of measurement accuracy, and gravity decreases were observed at some sites. We observed an obvious increase in gravity from January to March 2001, followed by a gravity decrease from March to May 2001. Overall, while gravity values rose steadily to November 2000, there were temporal fluctuations after December 2000.

[44] According to the volcano observations by JMA, the rate of SO_2 emission gradually decreased from 2001 to 2002, and at the time this paper was written remains at $1.0-2.0 \times 10^4$ t/d on average. After January 2001, however, small-scale summit eruptions occurred occasionally, with plume tops approaching 1000–2000 m above sea level and each eruption lasting at most 5–6 min. Eruptions occur roughly once or twice per month. The temperature close to the vent fluctuates between 100 and 400°C, and did not show any significant decreasing trend until 6 June 2001. Lower-frequency volcanic tremors have also been detected from January 2001.

[45] On the basis of the observations above, we can divide the temporal evolution after September 2000 into two substages; before and after January 2001. From January 2001, there have been occasional small eruptions and temporal fluctuations in gravity, and the physical state of the volcano appears to have changed. The interpretation and modeling results for the period after January 2001 will be reported elsewhere. In the following, we estimate the cumulative crustal displacements (Figures 11a and 11b), show the observed gravity changes (Figure 11c) and interpret these data for the period September to November 2000. As shown in Figure 3, the gradient of gravity and elevation changes is significantly greater than that of the free-air gradient.

7.2. Interpretation and Modeling

[46] Because caldera collapse had finished by September 2000, we can assume that the gravity changes in Figure 11c can be regarded to consist of the effects of crustal deformation and density changes beneath the ground. According to Figures 11a and 11b, the effect on gravity should be less than 20 μGal near the coastline. Using the subsidence rate at MYK1 as a proxy for that at the absolute gravity point and assuming 3.0 μGal/cm as the gravity gradient, the effect of ground subsidence for the 2.5 months would be 10.5 μGal. Considering the measurement accuracy of the absolute gravimeter, this value is significantly smaller than the observed changes of 19 μGal. It is therefore necessary to suppose unrealistically large values of either the subsidence rate or the gravity gradient to explain the changes in terms of ground subsidence alone. Hence the temporal gravity increase was presumed to be caused by crustal deformation and an increase in density beneath the volcano. The significant deviation of the relevant plots in Figure 3 from the free-air gradient also supports this interpretation.

[47] We interpret from the largest eruption on 18 August 2000 that the conduit from the chamber beneath the volcano was probably connected to the surface vent. Magma would then be able to rise through the conduit toward the surface

Table 2. Optimum Model Parameters for Figure 9

Parameter	Value
Deflation Source I	
Medium density,[a] kg/m³	2600
Longitude	139°31′47″ ± 5″
Latitude	34°3′53″ ± 5″
Depth (m)	3700 ± 100
Volume change, m³	$-1.6 \pm 0.5 \times 10^7$
Deflation Source II	
Medium density,[a] kg/m³	2600
Longitude	139°29′0″ ± 3″
Latitude	34°5′18″ ± 5″
Depth (m)	1900 ± 100
Volume change, m³	$-3.7 \pm 0.5 \times 10^6$
Cylindrical Body	
Longitude[b]	139°31′50″
Latitude[b]	34°5′1″
Bottom depth, m	2700 ± 300
Radius, m	235 ± 10
Vertical length, m	1000 ± 200
Density contrast, kg/m³	−1000 ± 300

[a]Density inside the source is fixed.
[b]Horizontal location of the cylinder is fixed beneath the collapsed caldera.
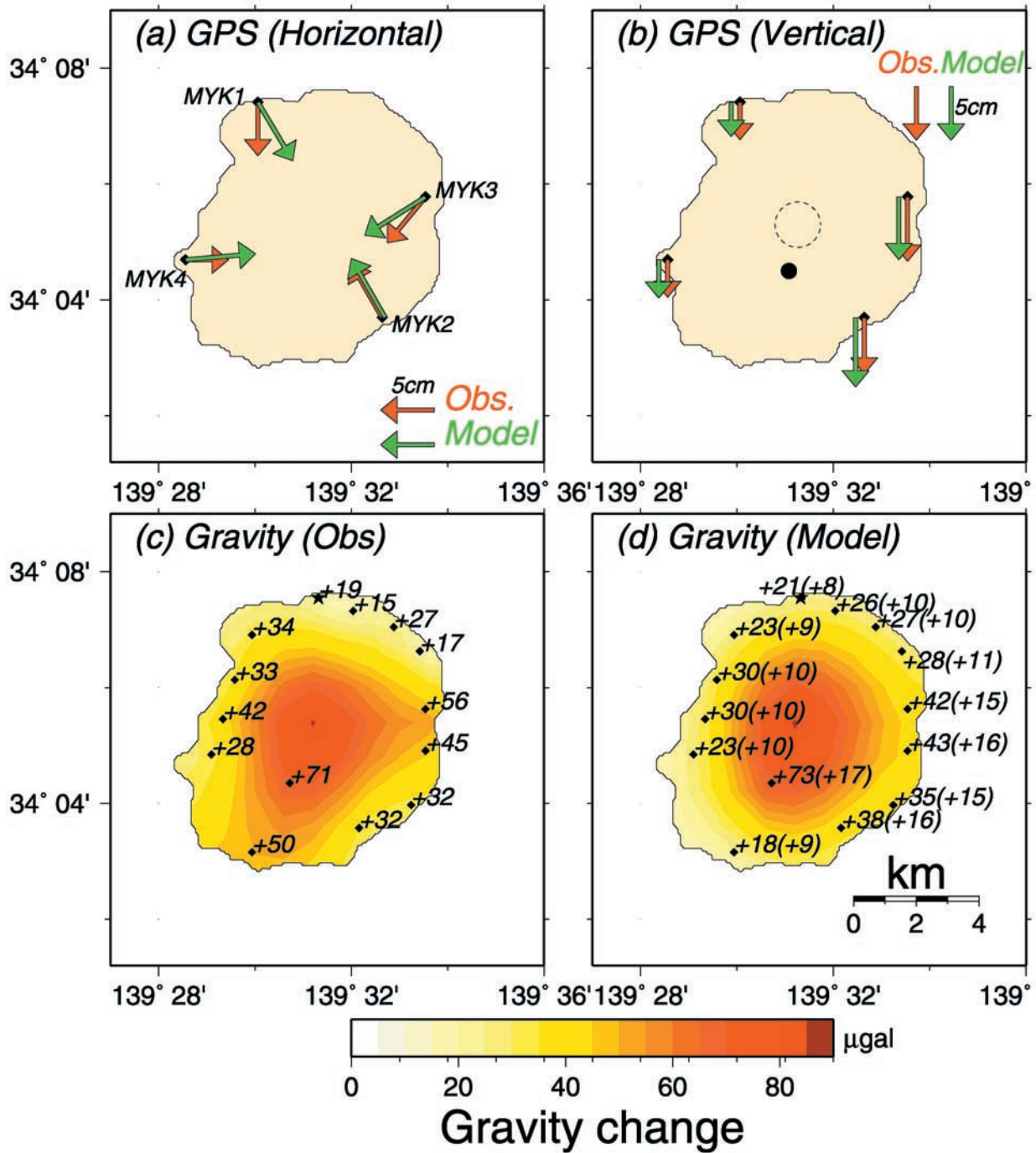
Figure 11. (a) Estimated horizontal ground displacement from September to November 2000. (b) Estimated vertical ground displacement. (c) Gravity changes acquired from 11–14 September to 10–12 November 2000. Units are in microGals. The reference site is located at the northern most point, as designated by a star. (d) Computed gravity changes based on optimum model. See Table 3. Numbers in parentheses show the contribution from the deflation source.

vent, causing both the temporal increase in temperature observed near the vent and the volcanic glow in December 2000. The upwelling magma is also considered to be responsible for the period of increased SO₂ emission from September to December 2000 and would have contributed to the increase in gravity values.

[48] We thus developed a model to explain both gravity changes and crustal deformation from September to

November 2000 and carried out a joint inversion as in previous sections. The weight is set at 10 μGal for the gravity data and 2 μGal for the absolute gravimeter. The weight for the GPS data is set at 5 cm, considering the errors in the estimate of ground displacement. The model consists of a cylindrical body as in Figure 10 and a deflation source. The latter element alone causes a contraction and a subsidence of the island. In contrast to the previous stages, the

Table 3. Optimum Model Parameters for Figure 11

Parameter	Value
Deflation Source	
Medium density,[a] kg/m^3	2600
Longitude	139°31′5″ ± 3″
Latitude	34°4′30″ ± 3″
Depth, m	5300 ± 1000
Volume change, m^3	−1.1 ± 0.5 × 10^7
Cylindrical Body	
Longitude[b]	139°31′50″
Latitude[b]	34°5′1″
Bottom depth,[c] m	2500 ± 300
Radius, m	125 ± 50
Density contrast,[b] kg/m^3	+1000

[a]Density inside the source is fixed.
[b]Horizontal location and density increase of a cylinder body are fixed.
[c]Top depth of cylinder body is assumed to correspond to sea level.

ground displacement after September 2000 indicates rather uniform contraction, and thus we prescribed a single deflation source. In view of the temporal increase in the corrected gravity from September 2000 (Figure 8), we interpret that the density increase occurred in the same region as the density decrease in the previous stage. Therefore the horizontal location of the cylindrical body is assumed to be the same as that in Table 2. Moreover, assuming that the density inside the conduit recovered from September 2000, the increase in density is assumed to be +1000 kg/m^3 in light of the density change estimated in section 7.1 (Table 2). We also suppose that a magma head was rising up to sea level and that an increase in density occurred from sea level to some unknown depth. We thus estimate the depth and volume change of the deflation source and the radius and depth of the cylindrical body.

[49] The computed changes for gravity and ground displacement are shown in Figures 11a, 11b, and 11d. The optimum parameters are listed in Table 3. The estimated radius and depth of the cylinder is in broad agreement with that estimated in the previous section (Table 2), suggesting that the model consistently describes the situation at Miyakejima in 2000. The numbers in parentheses in Figure 11d are the contribution from the deflation source alone. We see that the gravity increase after September 2000 was caused by a density increase in the cylindrical body, which may represent a magma refilling process.

8. Discussion
8.1. Mechanisms of Caldera Collapse

[50] Many calderas are considered to have formed as a result of collapse of the roof of the magma chamber [*Williams*, 1941], yet few such events have been witnessed historically [*Simkin and Howard*, 1970]. The caldera formation process at 2000 Miyakejima is the first caldera collapse to be monitored intensively by modern measurement instruments. In light of the gravity changes in Figure 4c, it is highly probable that an empty space formed prior to the caldera collapse. Total magnetic intensity data provide further evidence for the existence of an empty space [*Sasai et al.*, 2001]. This scenario also explains why the ground surface of the collapsed caldera on 9 July remained partially vegetated and why such a small volume of material was erupted.

[51] We then have to consider when and how the empty space was formed. Our speculative scenario is as follows. During the initial deflation of the magma chamber and subsequent dike intrusion, magma flowed out laterally from the magma chamber beneath Miyakejima to the offshore crust, causing the earthquake swarms. The direction of dike intrusion and the strike of the intense seismic swarms are perpendicular to the orientation of maximum tension stress in the oceanic crust [*Nakamura et al.*, 1984], reminiscent of the lateral magma flow characteristic in rift zone volcanoes [*Sigurdsson and Sparks*, 1978; *Rubin and Pollard*, 1987; *Lister and Kerr*, 1991; *Tilling and Dvorak*, 1993]. It is interesting that such a phenomenon occurred in an island arc volcano. We interpret that the voluminous lateral flow of magma broke the lithostatic balance between the magma chamber and surface crust, thereby forming a void in the topmost region of the magma chamber, causing the chamber roof to collapse (Figure 12b). We believe that the formation of this empty space immediately precipitated the collapse. The negative gravity changes detected on 6 July 2000 around the summit (Figure 4c) would therefore represent a snapshot of the upward propagating void, which eventually caused the small eruption on 8 July and collapse of the caldera. The dramatic increase in seismic activity immediately below the volcano from around 4 July 2000 presumably corresponds to the initiation of internal collapse.

[52] The reason for the large lateral magma flow may be as follows. It is generally accepted that there exists a level of neutral buoyancy (LNB) at which ascending magma is in gravitational equilibrium with the country rock. The high fracture resistance of the country rock allows the magma to pool at the LNB to form a magma chamber. Without the effect of fracture resistance, magma will not pool and will instead flow out laterally. The low viscosity of basaltic magma allows volatiles formed during crystallization of the magma to separate easily from the liquid, often triggering eruptions [*Tait et al.*, 1989; *Woods and Cardoso*, 1997]. The eruptions at Miyakejima over the past few centuries may have been caused by such mechanisms (Figure 12a). We conjecture that the residual, denser volatile-depleted liquid must have accumulated in the magma chamber, unable to descend because the liquid is still less dense than the underlying country rock. In such circumstances, the liquid magma tends to spread laterally, similar to dike intrusions in rift zones [*Rubin and Pollard*, 1987; *Lister and Kerr*, 1991], in mechanical balance with the fracture resistance of the country rock (Figure 12a). As the eruptions repeat many times, the volume of denser liquid will increase, and the magma pressure may exceed the critical fracture resistance of the country rock, allowing a lot of magma to flow out laterally. The recurrence period of caldera collapse may therefore be controlled by a balance between the fracture resistance and magma pressure, with the latter progressively increasing with repeated eruptions. The previous caldera formation event at the Miyakejima volcano is geologically estimated to be about 2500 years [*Tsukui and Suzuki*, 1998]. We can therefore expect to develop a more quantitative model that considers the numerous competing processes involved.

8.2. Explosive Basaltic Eruptions

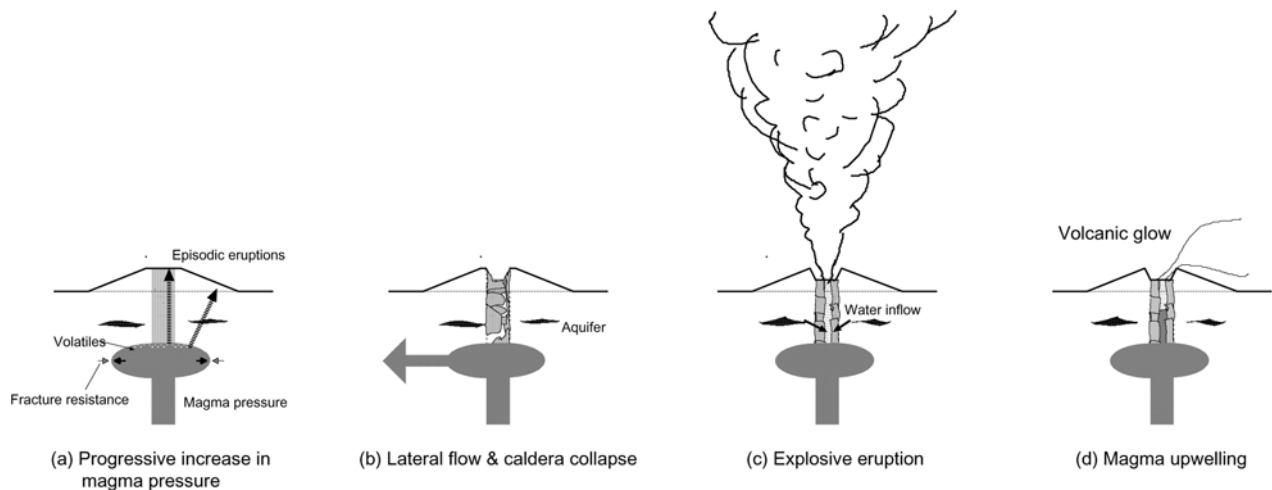[53] Eruptions of basaltic volcanoes are known to be less explosive than for silicic volcanoes, because the lower

Figure 12. Speculative scenario for the temporal evolution of unrest at the Miyakejima volcano. (a) Magma is in gravitational equilibrium at the level of neutral buoyancy, and the magma pressure is mechanically balanced with the fracture resistance of the country rock. Repeated episodic eruptions will progressively increase the volume of denser liquid and cause the magma pressure to exceed the fracture resistance of the country rock. (b) Lateral magma flow initiated internal collapse of a preexisting cylindrical structure and caldera collapse on the surface. (c) Explosive eruption due to intense interaction between magma and water from an ambient aquifer. (d) Magma ascent in the conduit. Volcanic gas emission rate increased, and night volcanic glow is observed. As time passes, the ascended magma cools and may eventually reach the initial stage.

viscosity of basaltic magma allows volatiles to segregate easily. As observed in the 1983 eruption of Miyakejima [*Aramaki et al.*, 1986], fire fountains and lava flows are also typical in basaltic eruptions. However, the summit eruptions since 14 July 2000 have been rather explosive. Neither fire fountains nor lava flows were observed in the 2000 eruptions at Miyakejima.

[54] There are a number of reports of explosive eruptions of basaltic volcanoes [*Decker*, 1987; *Walker et al.*, 1984; *Aramaki et al.*, 1986; *Dvorak*, 1992]. In each case, the explosivity is largely governed by interaction between surface water and magma [*Wohletz*, 1986; *Koyaguchi and Woods*, 1996]. The material erupted during the 2000 eruptions of Miyakejima was mostly fine ash [*Nakada et al.*, 2001], which was probably generated by intense magma-water interaction and subsequent magma fragmentation.

[55] The optimum cylinder model was developed to explain the spatiotemporal evolution of gravity (Figure 9c) and may reveal how the explosive eruptions were generated during the caldera collapse. In view of the inferred negative density contrast, we speculate that a preexisting cylindrical structure collapsed internally, and then began filling with water from the ambient aquifer. Hot magma then came into direct contact with the water, causing superheating and expansion of the liquid water in the collapsed cylinder (Figures 12b and 12c). The collapsed cylinder would eventually become incapable of sustaining high gas pressure, leading to the observed explosive eruptions (Figure 12c).

[56] After the largest eruption on 18 August 2000, an open conduit is expected to have formed. Magma could then ascend easily from the chamber, effectively bringing the lateral outflow to an end and increasing the local gravity

as noted above. As the magma head rose, the magma began to degas (Figure 12d). This process may be viewed as a refilling of the magma reservoir. Although not related to caldera collapse or explosive eruptions, *Dzurisin et al.* [1980] proposed a similar model to explain gravity changes associated with an *M* 7.2 earthquake at Kilauea volcano in 1975. Immediately following the earthquake, a void space was created beneath the summit area as a result of magma draining away into the rift zones. During the following 2 years, there were significant gravity increases in the absence of comparable height changes, interpreted as reflecting the refilling of voids with magma.

[57] *Decker* [1987] argued that on the basis of observations of Kilauea volcano, major explosive eruptions appear to be associated with caldera collapse. The 2000 unrest at Miyakejima could be viewed as such an example. The postulated mechanisms of caldera collapse and the explosive eruption at Miyakejima may be valid for all basaltic volcanoes regardless of tectonic environment.

9. Conclusion

[58] Employing both absolute and relative gravimeters, we have been recording the spatiotemporal evolution of the gravity field of the Miyakejima volcano in Japan since June 1998. The observed gravity changes provide us with strong evidence for the formation of an empty space beneath the island prior to summit collapse. The appreciable gravity changes immediately following the initiation of collapse can largely be explained by a collapsed topography model, involving an initially rapid rate of collapse without accompanying eruptions.

[59] Correcting for the gravity changes due to the caldera collapse at Miyakejima, we found a temporal decrease in gravity from July to late August 2000, coinciding with a period of intermittent explosive summit eruptions. This is modeled as a temporal reduction in density caused by water
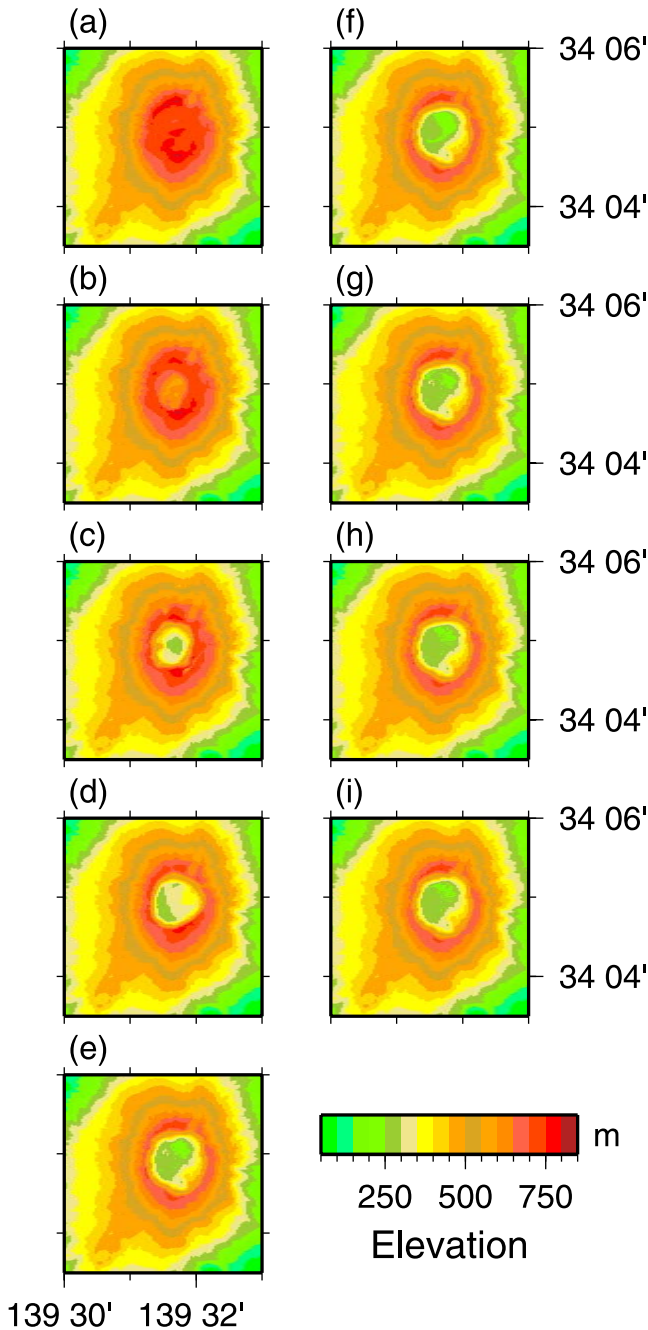
Table A1. Estimated Volume of Collapsed Caldera[a]

Measurement Date	This Study	GSI
9 July 2000	5.77	5.6
22 July 2000	28.0	26.5
2 Aug. 2000	43.4	42.6
28 Sept. 2000	61.2	60.0
6 Oct. 2000	62.1	-
8 Nov. 2000	62.4	-
30 Nov. 2000	62.5	-
16 Jan. 2001	62.7	-

[a]Units are in 10^7 m^3. Estimate by GSI is given for comparison [*Hasegawa et al.*, 2001].

inflow from an aquifer into the internally collapsing cylindrical space. We interpret that intense magma-water interaction caused the explosive summit eruptions. Since September 2000, gravity values have continued to increase despite only small ground displacements, interpreted as the refilling of magma into the conduit.

Appendix A

[60] Here we discuss the derivation of the synthesized DTM of the entire island (Figure A1). The mesh size of the DTM is 10 m, and the positioning error of the control point in the original GSI's DTM is about 3.5 m horizontally and 5.0 m vertically [*Hasegawa et al.*, 2001]. As recognized by GSI, however, there are spurious data in the vicinity of the caldera border, which obviously prevents us from using the original data as they are. Moreover, GSI's original DTMs for the collapsed area are only available for particular periods. The area covered therefore depends on the measurement period. In order to correct gravity values for the effect of temporal changes in topography, we need to use a DTM that records the temporal changes in topography as accurately as possible. We first synthesized the DTM for the entire island such that the caldera rim smoothly connects to the flank of the volcano, performed manually by visual inspection. Next we computed the effect of topography changes at each gravity site at the time of photogrammetry, the values of which are designated by circles in Figure 8. Here we used an analytical formula for the gravitational attraction of a rectangular parallelepiped [*Banerjee and Das Gupta*, 1977]. For the end-members of crustal density, we assumed 1900 and 2300 kg/m^3. We modeled the temporal evolution of caldera growth using an analytical form of $(1 - \exp(-t/\tau))$, and predicted gravity changes on those periods of gravity measurement. The time constant τ was estimated to be 22 days. For assessment of the accuracy of DTM, we show two independent estimates of cumulative collapsed volume in Table A1. The estimated volumes at each measurement date are within 5% of observed values, and the estimated volume after September 2000 is within 2% of observed values, demonstrating the accuracy of the model into the period after cessation of caldera collapse.

Figure A1. Temporal evolution of collapsed caldera at Miyakejima volcano. (a) Original topography of the summit area. Maps after the collapse of caldera are based on the synthetic DTM, for (b) 9 July 2000, (c) 22 July 2000, (d) 2 August 2000, (e) 28 September 2000, (f) 6 October 2000, (g) 8 November 2000, (h) 30 November 2000, and (i) 16 January 2001. (Copyright of original data is retained by the Geographical Survey Institute (GSI) of Japan; copyright of original data taken on 28 September 2000 is shared by GSI, NEC corporation, and HONDA Airways.)

References

Aramaki, S., Y. Hayakawa, T. Fujii, K. Nakamura, and T. Fukuoka, The October 1983 eruption of Miyakejima volcano, *J. Volcanol. Geotherm. Res.*, *29*, 203–229, 1986.

Banerjee, B., and S. P. Das Gupta, Gravitational attraction of a rectangular parallelepiped, *Geophysics*, *42*(5), 1053–1055, 1977.

Battaglia, M., G. Roberts, and P. Segall, Magma intrusion beneath Long Valley Caldera confirmed by temporal changes in gravity, *Science*, *285*, 2119–2122, 1999.

Berrino, G., H. Rymer, G. C. Brown, and G. Corrado, Gravity-height correlations for unrest at calderas, *J. Volcanol. Geotherm. Res.*, *53*, 11–26, 1992.

Decker, R. W., Dynamics of Hawaiian volcanoes: An overview, *U.S. Geol. Surv. Prof. Pap.*, *1350*, 997–1018, 1987.

Dvorak, J. J., Mechanism of explosive eruptions of Kilauea Volcano, Hawaii, *Bull. Volcanol.*, *54*, 638–645, 1992.

Dzurisin, D., L. A. Anderson, G. P. Eaton, R. Y. Koyanagi, R. T. Okamura, G. S. Puniwai, M. K. Sako, and K. M. Yamashita, Geophysical observations of Kilauea volcano, Hawaii: 2. Constraints on the magma supply during November 1975–September 1977, *J. Volcanol. Geotherm. Res.*, *7*, 241–269, 1980.

Fujii, T., and I. Kushiro, Density, viscosity, and compressibility of basaltic liquid at high pressures, *Yearb. Carnegie Inst. Washington*, 419–424, 1977.

Gottsmann, R., and H. Rymer, Deflation during caldera unrest: constraints on subsurface processes and hazard prediction from gravity-height data, *Bull. Volcanol.*, *64*, 338–348, 2002.

Hagiwara, Y., The Mogi model as a possible cause of the crustal uplift in the eastern part of Izu Peninsula and the related gravity change (in Japanese with English abstract), *Bull. Earthquake Res. Inst. Univ. Tokyo*, *52*, 301–309, 1977.

Hasegawa, H., M. Murakami, H. Masaharu, K. Matsuo, and M. Koarai, Caldera subsidence measurement at Miyakejima summit (in Japanese), *J. Geogr. Surv. Inst.*, *95*, 121–128, 2001.

Jachens, R. C., and G. P. Eaton, Geophysical observations of Kilauea Volcano, Hawaii: 1. Temporal gravity variations related to the 20 November, 1975, *M* = 7.2 earthquake and associated summit collapse, *J. Volcanol. Geotherm. Res.*, *7*, 225–240, 1980.

Japan Meteorological Agency, Recent seismic activity in the Miyakejima and Niijima-Kozushima region, Japan—The largest earthquake swarm ever recorded, *Earth Planets Space*, *52*, i–viii, 2000.

Kaidzu, M., T. Nishimura, M. Murakami, S. Ozawa, T. Sagiya, H. Yarai, and T. Imakiire, Crustal deformation associated with crustal activities in the northern Izu-islands area during the summer, 2000, *Earth Planets Space*, *52*, ix–xviii, 2000.

Kasahara, J., S. Nakao, and K. Koketsu, Tidal influence on the 2000 Miyake-jima eruption and its implications for hydrothermal activity and volcanism, *Proc. Jpn. Acad.*, *77B*, 98–103, 2001.

Kazahaya, K., J. Hirabayashi, H. Mori, M. Odai, Y. Nakahori, K. Nogami, S. Nakada, H. Shinohara, and K. Uto, Volcanic gas study of the 2000 Miyakejima volcanic activity: Degassing environment deduced from adhered gas component on ash and SO_2 emission rate (in Japanese with English abstract), *J. Geogr.*, *110*(2), 271–279, 2001.

Koyaguchi, T., and A. W. Woods, On the formation of eruption columns following explosive mixing of magma and surface-water, *J. Geophys. Res.*, *101*, 5561–5574, 1996.

Kumagai, H., T. Ohminato, M. Nakano, M. Ooi, A. Kubo, H. Inoue, and J. Oikawa, Very-long-period seismic signals and caldera formation at Miyake Island, Japan, *Science*, *293*, 687–690, 2001.

Lister, J. R., and R. C. Kerr, Fluid-mechanical models of crack propagation and their application to magma transport in dikes, *J. Geophys. Res.*, *96*, 10,049–10,077, 1991.

Miyazaki, T., Features of historical eruptions at Miyake-jima Volcano (in Japanese with English abstract), *Bull. Volcanol. Soc. Jpn.*, *11*, S1–S15, 1984.

Mogi, K., Relations between the eruptions of various volcanoes and deformations of the ground surfaces around them, *Bull. Earthquake Res. Inst. Univ. Tokyo*, *36*, 99–134, 1958.

Nakada, S., M. Nagai, A. Yasuda, T. Shimano, N. Geshi, M. Ohno, T. Akimasa, T. Kaneko, and T. Fujii, Chronology of the Miyakejima 2000 eruption: Characteristics of summit collapsed crater and eruption products (in Japanese with English abstract), *J. Geogr.*, *110*(2), 168–180, 2001.

Nakamura, K., K. Shimazaki, and N. Yonekura, Subduction, bending and eduction: Present and Quaternary tectonics of northern border of the Philippine Sea Plate, *Bull. Soc. Geol. Fr.*, *26*(2), 221–243, 1984.

Niebauer, T. M., G. Sasagawa, J. E. Faller, R. Hilt, and F. J. Klopping, A new generation of absolute gravimeters, *Metrologia*, *32*, 159–180, 1995.

Nishimura, T., S. Ozawa, M. Murakami, T. Sagiya, T. Tada, M. Kaidzu, and M. Ukawa, Crustal deformation caused by magma migration in the northern Izu Islands, Japan, *Geophys. Res. Lett.*, *28*, 3745–3748, 2001.

Okada, Y., Surface deformation due to shear and tensile faults in a half-space, *Bull. Seismol. Soc. Am.*, *75*, 1135–1154, 1985.

Okubo, S., Potential and gravity changes due to shear and tensile faults in a half-space, *J. Geophys. Res.*, *97*, 7137–7144, 1992.

Okubo, S., and H. Watanabe, Gravity change caused by a fissure eruption, *Geophys. Res. Lett.*, *16*, 445–448, 1989.

Press, W. H., B. P. Flannery, S. A. Teukolsky, and W. T. Vetterling, *Numerical Recipes in C: The Art of Scientific Computing*, 2nd ed., 994 pp., Cambridge Univ. Press, New York, 1992.

Rubin, A. M., and D. D. Pollard, Origins of blade-like dikes in volcanic rift zones, *U.S. Geol. Surv. Prof. Pap.*, *1350*, 1449–1470, 1987.

Rymer, H., J. Cassidy, C. A. Locke, and J. B. Murray, Magma movements in Etna volcano associated with the major 1991–1993 lava eruption: Evidence from gravity and deformation, *Bull. Volcanol.*, *57*, 451–461, 1995.

Sakai, S., Seismicity nearby Miyake-jima and Kozu-shima Island (in Japanese), *KOHO 30*, pp. 5–7, Earthquake Res. Inst., Univ. of Tokyo, Tokyo, 2000.

Sakai, S., et al., Magma migration from the point of view of seismic activity in the volcanism of Miyake-jima Island in 2000 (in Japanese with English abstract), *J. Geogr.*, *110*(2), 145–155, 2001.

Sasai, Y., M. Uyeshima, H. Utada, T. Kagiyama, J. Zlotnicki, T. Hashimoto, and Y. Takahashi, The 2000 activity of Miyake-jima Volcano as inferred from electric and magnetic field observations, *J. Geogr.*, *110*(2), 226–244, 2001.

Sigurdsson, H., and S. R. J. Sparks, Lateral magma flow within rifted Iceland crust, *Nature*, *274*, 126–130, 1978.

Simkin, T., and K. A. Howard, Caldera collapse in the Galapagos Islands, 1968, *Science*, *169*, 429–437, 1970.

Singh, S. K., Gravitational attraction of a vertical right circular cylinder, *Geophys. J. R. Astron. Soc.*, *50*, 243–246, 1977.

Tait, S., C. Jaupart, and S. Vergniolle, Pressure, gas content and eruption periodicity of a shallow, crystallising magma chamber, *Earth Planet. Sci. Lett.*, *92*, 107–123, 1989.

Tanaka, Y., S. Okubo, M. Machida, I. Kimura, and T. Kosuge, First detection of absolute gravity change caused by earthquake, *Geophys. Res. Lett.*, *28*, 2979–2981, 2001.

Tilling, R. I., and J. J. Dvorak, Anatomy of a basaltic volcano, *Nature*, *363*, 125–133, 1993.

Tokyo Metropolitan Government, Research report on the characteristics of volcanic eruptions in Izu-islands (Miyakejima) (in Japanese), 103 pp., Tokyo Metrop. Govt. Disaster Prevent. Congr., Tokyo, 1990.

Tsukui, M., and M. Suzuki, Eruptive history of Miyakejima Volcano during the last 7000 years (in Japanese with English abstract), *Bull. Volcanol. Soc. Jpn.*, *43*, 149–166, 1998.

Ukawa, M., E. Fujita, E. Yamamoto, Y. Okada, and M. Kikuchi, The 2000 Miyakejima eruption: Crustal deformation and earthquakes observed by the NIED Miyakejima observation network, *Earth Planets Space. 52*, xix–xxvi, 2000.

Walker, G. P. L., S. Self, and L. Wilson, Tarawera 1886, New Zealand—A basaltic Plinian fissure eruption, *J. Volcanol. Geotherm. Res.*, *21*, 61–78, 1984.

Wessel, P., and W. H. F. Smith, New, improved version of Generic Mapping Tools released, *Eos Trans. AGU*, *79*(47), 579, 1998.

Williams, H., Calderas and their origin, *Bull. 25*, pp. 239–346, Univ. of Calif., Dep. of Geol. Sci., Berkeley, 1941.

Wohletz, K. H., Explosive magma-water interactions: Thermodynamics, explosion mechanisms, and field studies, *Bull. Volcanol.*, *48*, 245–264, 1986.

Woods, A. W., and S. S. S. Cardoso, Triggering basaltic volcanic eruptions by bubble-melt separation, *Nature*, *385*, 518–520, 1997.

————————————

M. Furuya, J. Oikawa, S. Okubo, W. Sun, Y. Tanaka, and H. Watanabe, Earthquake Research Institute, University of Tokyo, Yayoi 1-1-1, Bunkyo-ku, Tokyo 113-0032, Japan. (furuya@eri.u-tokyo.ac.jp; oikawa@eri.u-tokyo.ac.jp; okubo@eri.u-tokyo.ac.jp; sunw@eri.u-tokyo.ac.jp; ytanaka@eri.u-tokyo.ac.jp; watanabe@eri.u-tokyo.ac.jp)

T. Maekawa, Graduate School of Science, Hokkaido University, Tatsuka 142, Sobetsu-cho, Usu-gun, Hokkaido 052-0106, Japan. (maekawa@uvo.sci.hokudai.ac.jp)